

Charge density distributions and related form factors in neutron-rich light exotic nuclei

A.N. Antonov^{a,b}, M.K. Gaidarov^a, D.N. Kadrev^a,
P.E. Hodgson^c, E. Moya de Guerra^d

^a*Institute of Nuclear Research and Nuclear Energy,
Bulgarian Academy of Sciences, Sofia 1784, Bulgaria*

^b*Departamento de Fisica Atomica, Molecular y Nuclear,
Facultad de Ciencias Fisicas, Universidad Complutense de Madrid,
Madrid E-28040, Spain*

^c*Subdepartment of Particle Physics, Department of Physics,
University of Oxford, Oxford OX1-3RH, United Kingdom*

^d*Instituto de Estructura de la Materia, CSIC, Serrano 123,
28006 Madrid, Spain*

Charge form factors corresponding to proton density distributions in exotic nuclei, such as ${}^6,8\text{He}$, ${}^{11}\text{Li}$, ${}^{17,19}\text{B}$ and ${}^{14}\text{Be}$ are calculated and compared. The results can be used as tests of various theoretical models for the exotic nuclei structure in possible future experiments using a colliding electron-exotic nucleus storage ring. The result of such a comparison would show the effect of the neutron halo or skin on the proton distributions in exotic nuclei.

1 Introduction

It has been shown (see, e.g. the review [1]) that the study of exotic nuclei is likely to reveal new aspects of nuclear structure. Since the first experiments with radioactive nuclear beams (RNB) took place (e.g. [2]) it has been found from analyses of the total interaction cross sections that weakly-bound nuclei have increased sizes that deviate substantially from the $R \sim A^{-1/3}$ rule. It became clear (e.g. [3, 4]) that such new phenomena are due to the weak binding of the last few nucleons which form a diffuse nuclear cloud due to quantum-mechanical penetration (the so called nuclear halo). Another effect is that the nucleons can form a neutron skin [5] when the neutrons are on average less bound than the protons. Most of the neutron haloes have been studied for the lightest elements, such as He, Li, Be, B and other isotopes.

Direct reactions are a well-known tool to provide information on nuclear structure. Most exotic nuclei are so shortlived that they cannot be used as targets. Instead, direct reactions with RNB can be done in inverse kinematics where the role of beam and target are interchanged. For example, the proton elastic-scattering angular distributions were measured for several incident energies, namely 25.1A MeV [6, 7], 41.6A MeV [8, 9, 10] and 71A MeV [11, 12] for ${}^6\text{He}$, 26.25A MeV (the preliminary data obtained in Dubna [13]), 32A MeV [11, 12], 66A MeV [11, 12] and 73A MeV [11, 12, 14, 15] for ${}^8\text{He}$, as well as for energies less than 100A MeV [11, 1] in the cases of ${}^6\text{Li}$, ${}^{11}\text{Li}$ and others. In some of the theoretical analyses (e.g. [11, 12, 14, 16]) the eikonal approach using neutron and proton density distributions as well as parametrized nucleon-nucleon total cross sections have been used. The real part of the optical potential for calculations of ${}^6\text{He}+p$, ${}^6\text{He}+{}^4\text{He}$ ($E_{lab}=151$ MeV) [17] and ${}^6\text{He}+p$, ${}^8\text{He}+p$ ($E_{inc} < 100A$ MeV)

[18] elastic scattering angular distributions was obtained microscopically using the realistic M3Y-Paris effective interaction [19, 20, 21] as well as the Tanihata neutron and proton densities of helium isotopes [22] in [17, 18] and the densities derived from the cluster-orbital shell model approximation (COSMA) [23, 11, 12, 24] in [18]. It was shown that elastic scattering is a good tool to distinguish between different density distributions [18]. The results of [18] were compared also with those from the alpha-core approach with the complex and fully non-local effective interaction [25] and the no-core model based on the large space shell-model calculations (LSSM) ([26, 9, 27] and refs. therein). For larger energies (> 500 MeV/nucleon) it is accepted that the Glauber approximation is a suitable method to study charge and matter distributions from proton elastic scattering data [1, 28].

As mentioned in [1], however, an accurate determination of charge distributions of exotic nuclei can be obtained from electron-nucleus scattering in inverse kinematics using a colliding electron-exotic nucleus storage ring.

The aim of the present paper is to calculate the charge form factors of exotic nuclei such as ${}^6\text{He}$, ${}^8\text{He}$, ${}^{11}\text{Li}$, ${}^{17}\text{B}$, ${}^{19}\text{B}$ and ${}^{14}\text{Be}$ on the basis of charge density distributions calculated by using various theoretical models. This work can serve as a challenge for future experimental works on measurements of the charge form factors and thus for accurate determination of the charge distributions in these nuclei. The latter can be a test of the different theoretical models used for obtaining charge distributions. Second, this work can throw light on the question about the effect of the neutron halo or skin on the proton distributions in the helium, lithium, boron and beryllium isotopes.

A brief representation of the theoretical scheme is given in Sec. II. The results and discussion are presented in Sec. III.

2 The theoretical scheme

The charge form factor $F_{ch}(\mathbf{q})$ is the Fourier transform of the charge density distribution $\rho_{ch}(\mathbf{r})$:

$$F_{ch}(\mathbf{q}) = \int d\mathbf{r} \rho_{ch}(\mathbf{r}) e^{i\mathbf{q}\mathbf{r}} \frac{1}{\int \rho_{ch}(\mathbf{r}) d\mathbf{r}}. \quad (1)$$

Let us firstly consider $\rho_{ch}(\mathbf{r})$ obtained from a total nuclear wave function in which the positions \mathbf{r} of the nucleons are defined with respect to the centre-of-mass of the nucleons in the nucleus (c.m.). If the charge density is spherically symmetrical and normalized to unity, then:

$$F_{ch}(\mathbf{q}) = 4\pi \int \rho_{ch}(r) j_0(qr) r^2 dr, \quad (2)$$

where $j_0(qr)$ is the zero-order spherical Bessel function. Neglecting the charge neutron form factor, the charge density $\rho_{ch}(\mathbf{r})$ is represented by the density distribution of point-like protons in the nucleus $\rho_{point}(\mathbf{r})$ folded with the charge distribution of the proton $\rho_{pr}(\mathbf{r})$:

$$\rho_{ch}(\mathbf{r}) = \int \rho_{point}(\mathbf{r} - \mathbf{r}') \rho_{pr}(\mathbf{r}') d\mathbf{r}'. \quad (3)$$

Then the charge form factor (2) can be obtained in the form:

$$F_{ch}(\mathbf{q}) = F_{point}(\mathbf{q}) F_{pr}(\mathbf{q}), \quad (4)$$

where $F_{point}(\mathbf{q})$ and $F_{pr}(\mathbf{q})$ are the form factors which correspond to the densities $\rho_{point}(\mathbf{r})$ and $\rho_{pr}(\mathbf{r})$ (in formulae such as Eq. (2)), respectively. Secondly, in some calculations the wave functions which lead to the density distributions are often translationally non-invariant and the positions of the nucleons are determined with respect to the centre of the potential related to the

laboratory system (lab.) but not to the centre-of-mass of the nucleons in the nucleus. These wave functions admit a motion of the centre-of-mass which has to be switched off in the calculations. It is shown (e.g. in [29, 30, 31]) that the relationship between the form factor calculated by means of harmonic-oscillator wave functions (with all the nucleons in the $1s$ state) $F_{point,lab}(\mathbf{q})$ and the form factor calculated by actual wave functions (with positions of the nucleons determined in the c.m. system) $F_{point,c.m.}(\mathbf{q})$ contains a correction factor:

$$F_{point,c.m.}(\mathbf{q}) = e^{(qb)^2/4A} F_{point,lab}(\mathbf{q}), \quad (5)$$

where b is the harmonic-oscillator parameter, or

$$F_{point,c.m.}(\mathbf{q}) = e^{(qR)^2/6A} F_{point,lab}(\mathbf{q}), \quad (6)$$

R being the root-mean-square (rms) radius of the nucleus. For shell-model potentials different from the harmonic-oscillator one the Eqs. (5) and (6) are approximate. Thus in this case the expression for the form factor which can be compared with the experimental form factor can be written in the form [31]:

$$F_{ch}(\mathbf{q}) = e^{(qR)^2/6A} F_{point,lab}(\mathbf{q}) F_{pr}(\mathbf{q}). \quad (7)$$

In the Eqs. (1), (2), (4) and (7) all form factors are equal to unity at $\mathbf{q}=0$.

3 Results and discussion

In this Section we calculate $F_{point}(\mathbf{q})$ using the point charge density $\rho_{point}(\mathbf{r})$ in Eq. (2) and $F_{ch}(\mathbf{q})$ using Eq. (4) for the exotic nuclei ${}^6,8\text{He}$, ${}^{11}\text{Li}$, ${}^{14}\text{Be}$ and ${}^{17,19}\text{B}$. For comparison we present also the charge form factors of the "non-exotic" ${}^4\text{He}$ and ${}^6\text{Li}$ nuclei.

Various charge distributions of the proton $\rho_{pr}(\mathbf{r})$ can be used in order to obtain the form factor $F_{pr}(\mathbf{q})$. We use the Gaussian form normalized to unity:

$$\rho_{pr}(r) = \frac{1}{(\pi\alpha^2)^{3/2}} \exp(-r^2/\alpha^2) \quad (8)$$

which leads to the proton form factor

$$F_{pr}(\mathbf{q}) = e^{-q^2\alpha^2/4}. \quad (9)$$

For the value of the parameter α we choose $\alpha = 0.6532$ fm which corresponds to the proton rms radius $R_p = 0.80$ fm [32].

3.1 Density distributions of ${}^{4,6,8}\text{He}$

We use firstly the following point nucleon densities $\rho_{point}(r)$ for ${}^{4,6,8}\text{He}$ deduced by Tanihata et al. [22] which determine $F_{point}(\mathbf{q})$ in Eq. (4):

$$\rho_{point}^X(r) = \frac{2}{\pi^{3/2}} \left\{ \frac{1}{a^3} \exp \left[- \left(\frac{r}{a} \right)^2 \right] + \frac{1}{b^3} \frac{X-2}{3} \left(\frac{r}{b} \right)^2 \exp \left[- \left(\frac{r}{b} \right)^2 \right] \right\}, \quad (10)$$

where $X = Z, N$. These densities were obtained by fitting the measured total reaction cross sections of ${}^{4,6,8}\text{He}$ at 800A MeV incident on the C target using the optical limit of the Glauber model [33]. The parameter values a and b are determined from:

$$a^2 = a^{*2} \left(1 - \frac{1}{A} \right), \quad b^2 = b^{*2} \left(1 - \frac{1}{A} \right), \quad (11)$$

where $a^* = 1.53$ fm for all ${}^4, {}^6, {}^8\text{He}$ isotopes, $b^* = 2.24$ fm for ${}^6\text{He}$ and $b^* = 2.06$ fm for ${}^8\text{He}$ [22]. Hence, $a = 1.40$ fm and $b = 2.04$ fm for ${}^6\text{He}$, $a = 1.43$ fm and $b = 1.93$ fm for ${}^8\text{He}$ and $a = 1.325$ fm for ${}^4\text{He}$. Thus, the rms radii of the point-proton density distributions are 1.62 fm, 1.72 fm and 1.76 fm for ${}^4\text{He}$, ${}^6\text{He}$ and ${}^8\text{He}$, respectively.

We use secondly the COSMA point nucleon densities [24] of ${}^6, {}^8\text{He}$ which have the same analytical form (10) and are based on the assumption of the $1p_{3/2}$ state for the relative motion of the alpha-core and each of the valence neutrons. The parameter values are [11, 12] $a = 1.55$ fm, $b = 2.24$ fm for ${}^6\text{He}$ and $a = 1.38$ fm, $b = 1.99$ fm for ${}^8\text{He}$. The rms radii of the point-proton density distributions are 1.89 fm and 1.69 fm for ${}^6\text{He}$ and ${}^8\text{He}$, respectively. Here we would like to note the different trend in the behavior of the rms radii of the point-proton density distributions in the Tanihata density [22] and COSMA density [24, 11, 12]. While in the former the rms radius increases from ${}^4\text{He}$ to ${}^6\text{He}$ and ${}^8\text{He}$, in the latter it decreases from ${}^6\text{He}$ to ${}^8\text{He}$. Thus both densities contain opposite effects of the additional neutrons on the charge distributions in the helium isotopes. We note also that both Tanihata and COSMA densities have a Gaussian asymptotic behavior which is supposed not to be a realistic one for these nuclei at high q . Both densities had been used to fit mainly the total reaction cross sections and the rms radii. That is why it is necessary to consider also other more realistic theoretical predictions for the densities of the helium isotopes. We use also the proton densities of ${}^4, {}^6, {}^8\text{He}$ obtained within the LSSM calculations in a complete $4\hbar\omega$ shell-model space [26]. In them Woods-Saxon single-particle (s.p.) wave functions have been used for ${}^6\text{He}$ and ${}^8\text{He}$ and harmonic-oscillator ones for ${}^4\text{He}$. We use also the experimental charge density for ${}^4\text{He}$ [34] with charge rms radius equal to 1.696(14) fm.

3.2 Density distributions of ${}^6\text{Li}$ and ${}^{11}\text{Li}$

The COSMA point nucleon densities used in our calculations for ${}^6\text{Li}$ and ${}^{11}\text{Li}$ can be written in the following form [11]:

$$\rho_{point}^X(r) = N_{cX} \frac{\exp(-r^2/a^2)}{\pi^{3/2}a^3} + N_{\nu X} \frac{2 \exp(-r^2/b^2)}{3\pi^{3/2}b^5} \left[Ar^2 + \frac{B}{b^2} \left(r^2 - \frac{3}{2}b^2 \right)^2 \right], \quad X = Z, N. \quad (12)$$

For ${}^6\text{Li}$ (in the $\alpha+2N$ model): $A=1$, $B=0$, $N_{cZ} = N_{cN} = 2$, $N_{\nu N} = N_{\nu Z} = 1$, $a=1.55$ fm and $b=2.07$ fm [12]. For ${}^{11}\text{Li}$ (in the ${}^9\text{Li}+2N$ model): $A=0.81$, $B=0.19$, $N_{cZ} = 3$, $N_{cN} = 6$, $N_{\nu Z} = 0$, $N_{\nu N} = 2$, $a=1.89$ fm and $b=3.68$ fm [11]. The rms radii of protons are 2.44 fm and 2.31 fm for ${}^6\text{Li}$ and ${}^{11}\text{Li}$, respectively. Similarly to the case of the helium isotopes, the COSMA density predicts a decrease of the proton rms radius from ${}^6\text{Li}$ to ${}^{11}\text{Li}$ when the number of neutrons increases. Secondly, we use the proton density of ${}^6\text{Li}$ obtained within a LSSM in a complete $4\hbar\omega$ shell-model space and of ${}^{11}\text{Li}$ in a complete $2\hbar\omega$ shell-model calculations [35]. For ${}^{11}\text{Li}$ Woods-Saxon s.p. wave functions have been used and harmonic-oscillator ones for ${}^6\text{Li}$. Third, for ${}^6\text{Li}$ we use as well the density distribution of point-like protons [36, 37] which leads to the experimental charge distribution with rms radius equal to 2.57 fm [36].

3.3 Density distributions of ${}^{17,19}\text{B}$ and ${}^{14}\text{Be}$

The point nucleon distributions in ${}^{17,19}\text{B}$ and ${}^{14}\text{Be}$ were determined in [38] from analyses of the interaction cross sections of light radioactive nuclei close to the neutron drip line measured at around 800A MeV using the optical limit to Glauber type calculations by employing a harmonic-oscillator type densities including the contribution from the sd -shell:

$$\rho_{point}^Z(r) = \frac{2}{\pi^{3/2}\lambda^3} \frac{1}{\left(1 - \frac{1}{A}\right)^{3/2}} \exp(-x^2) \left[1 + \frac{(Z-2)}{3}x^2 \right], \quad (13)$$

$$\rho_{point}^N(r) = \frac{4}{\pi^{3/2}\lambda^3} \frac{1}{\left(1 - \frac{1}{A}\right)^{3/2}} \frac{N}{(N+8)} \exp(-x^2) \left[1 + 2x^2 + \frac{(N-8)}{15}x^4\right], \quad (14)$$

where

$$x^2 = \left(\frac{r}{\lambda}\right)^2 \frac{A}{A-1} \quad (15)$$

and λ is the width parameter. Its values are determined by a fit to the experimental interaction cross sections [38, 2]. In our work we use the values of λ which correspond to the values of the effective rms radii of the point nucleon distributions obtained in [38]. They are 1.9366 fm, 2.0365 fm and 2.0218 fm for ^{17}B , ^{19}B and ^{14}Be , respectively. The rms radii of the proton distributions are correspondingly 2.722 fm, 2.872 fm and 2.755 fm for ^{17}B , ^{19}B and ^{14}Be . Similarly to the case of the Tanihata densities of the helium isotopes the proton rms radius increases from ^{17}B to ^{19}B .

3.4 Results of calculations

In this subsection we present and compare the charge form factors $F_{ch}(q)$ for different nuclei calculated using Eq. (4) (which accounts for the proton size and in which the positions of the protons are determined from the centre-of-mass of the nucleons in the nucleus) and also make a comparison in one case with a form factor for point-like protons.

In Fig. 1 are compared the charge form factors $F_{ch}(q)$ (4) of ^6He and ^8He calculated using the Tanihata [22] and the COSMA [11] densities. For comparison are given the charge form factors for ^4He calculated using the experimental charge distribution from [34] and the Tanihata density [22]. In Fig. 2 the charge form factors for $^{4,6,8}\text{He}$ calculated using the LSSM densities [26] are compared with those for ^4He calculated with the experimental $\rho_{ch}(r)$ [34] and with the Tanihata density [22]. In Fig. 3 the charge form factors from (4) for ^6Li and ^{11}Li calculated using the COSMA densities [11, 12] are given together with those from calculations using the LSSM proton densities [35]. For comparison are given the charge form factors for ^6Li calculated using the experimental charge distribution from [36, 37] as well as the point-proton form factor for ^{11}Li calculated with the COSMA density distribution. The charge form factors of ^{17}B and ^{19}B are compared in Fig. 4 with that of ^{14}Be using Eq. (4) and the point-proton densities from [38]. The charge rms radii and the diffuseness parameters of the charge densities are given in Table 1. The diffuseness parameter is defined as the distance over which the value of $\rho_{ch}(r)$ decreases from 90% to 10% of the value of the density in the centre of the nucleus $\rho_{ch}(r=0)$ divided by 4.4.

3.5 Discussion and conclusions

The main features of the obtained charge form factors can be summarized as follows:

Although the number of the protons within a given group of isotopes is the same, the charge form factors are quite different from each other. This concerns $^{4,6,8}\text{He}$ nuclei (using the Tanihata, the COSMA and the LSSM densities), ^6Li and ^{11}Li (using the COSMA and the LSSM densities), as well as ^{17}B and ^{19}B isotopes (using the Suzuki densities). These differences reflect the differences in the phenomenologically obtained proton density distributions (which have been fitted to the empirical data for the total reaction cross sections) and in the corresponding radii. Thus the charge form factors can show the effects of the different number of neutrons and their distribution in the nucleus on the charge distribution in a given group of isotopes. Indeed, e.g. ^4He is a strongly bound α -cluster, while ^6He is a loosely bound $\alpha+n+n$ system. ^6Li is predominantly an $\alpha+d$ formation while ^{11}Li is supposed to be a $^9\text{Li}+n+n$ system. We should emphasize, however, the different trend of the behavior of the charge form factors for ^6He and ^8He when using the Tanihata, the COSMA and the LSSM densities. This follows, as

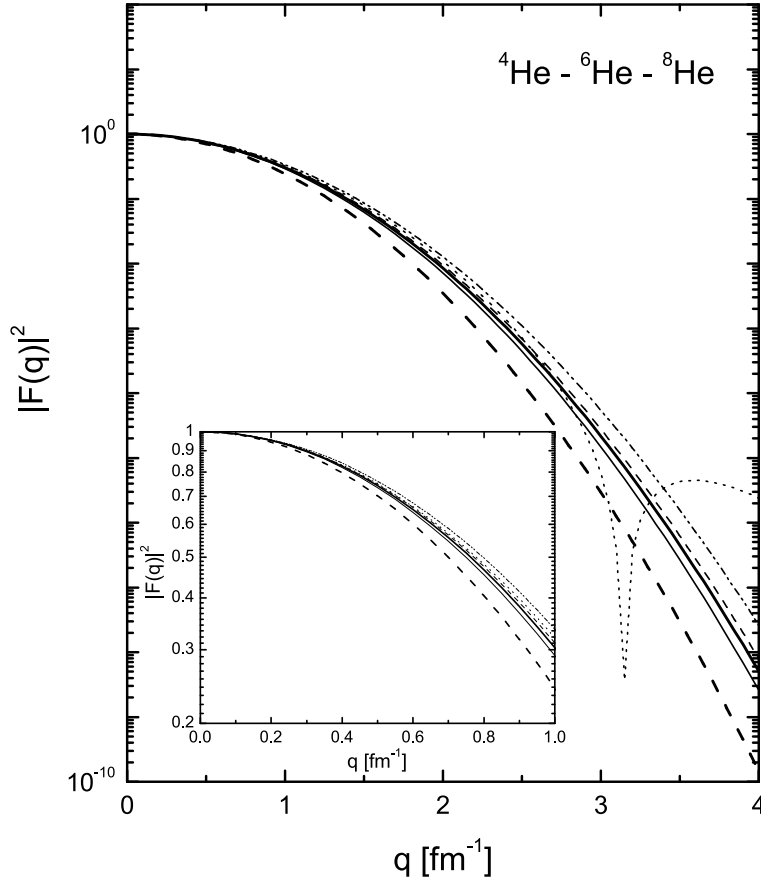


Figure 1: Charge form factors from Eq. (4): a) for ${}^4\text{He}$ calculated with the experimental $\rho_{ch}(r)$ [34] (dotted line) and with the Tanihata density [22] (dash-two-dotted line); b) for ${}^6\text{He}$ calculated using the Tanihata [22] (thick solid line) and the COSMA [11] (thick dashed line) densities, and c) for ${}^8\text{He}$ calculated using the Tanihata [22] (thin solid line) and the COSMA [11] (thin dashed line) densities.

can be expected, the changes of the proton rms radii (i.e. the changes of the neutron effect on the charge distributions) within a given theoretical approach. While in the case of the Tanihata density the proton rms increases from 1.72 fm for ${}^6\text{He}$ to 1.76 fm for ${}^8\text{He}$, in the COSMA and LSSM cases it decreases from 1.89 fm to 1.69 fm (in COSMA) and from 1.95 fm to 1.92 fm (in LSSM) for ${}^6\text{He}$ and ${}^8\text{He}$.

We should mention that the Tanihata, COSMA and Suzuki densities used in our work have Gaussian asymptotic behavior which is supposed not to be a realistic one for the nuclei considered at high q . This imposes the usage of other more realistic theoretical densities that may become available. We used the LSSM ones for ${}^4,6,8\text{He}$ and ${}^6,11\text{Li}$ nuclei. For ${}^6\text{He}$, ${}^8\text{He}$ and ${}^{11}\text{Li}$ Woods-Saxon s.p. wave functions have been used in the LSSM calculations.

We note also the important effect of the proton size accounted for in the calculations of the charge form factors.

In summary, various existing models of charge densities for light exotic nuclei differ very much in their form factor predictions. They even predict opposite effects of the neutron excess on the charge distribution that could be tested by measuring charge form factors. Therefore, it would be most desirable to compare the form factors obtained here with the future experimental data on electron-exotic nuclei scattering. Our numerical results for the charge form factors are available upon demand.

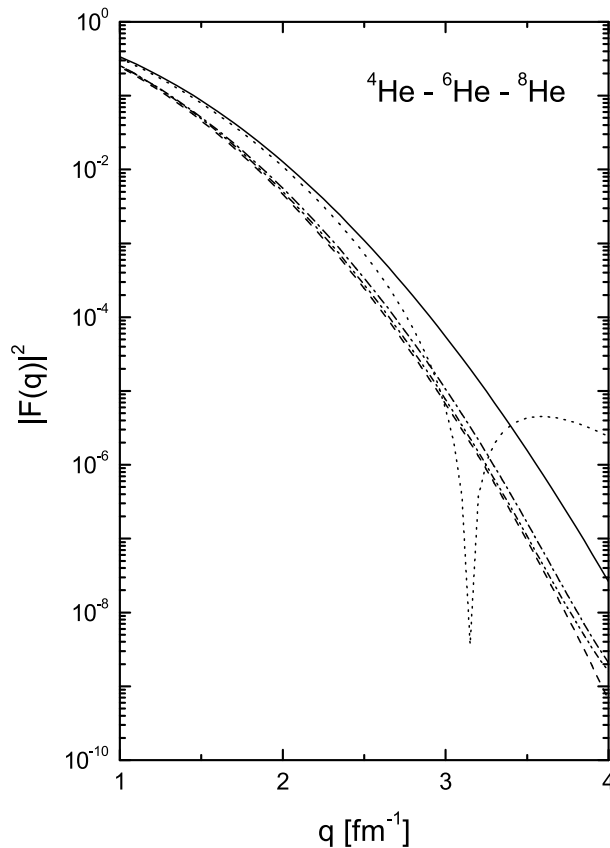


Figure 2: Charge form factors for $q \geq 1 \text{ fm}^{-1}$ from Eq. (4): a) for ${}^4\text{He}$ calculated with the experimental $\rho_{ch}(r)$ [34] (dotted line), with the Tanihata density [22] (solid line) and using the LSSM density [26] (dashed line); b) for ${}^6\text{He}$ calculated using the LSSM density [26] (dash-dotted line), and c) for ${}^8\text{He}$ calculated using the LSSM density [26] (dash-two-dotted line).

4 Acknowledgments

One of the authors (A.N.A.) thanks the Royal Society of London and the Bulgarian Academy of Sciences for support during his visit to the University of Oxford. He is also grateful for warm hospitality to the Faculty of Physics of the Complutense University of Madrid and for support during his stay there to the State Secretariat of Education and Universities of Spain (N/Ref. SAB2001 - 0030). Three of the authors (A.N.A., M.K.G. and D.N.K.) are grateful to the Bulgarian National Science Foundation for partial support under the Contract No. Φ -905.

References

- [1] R.F. Casten and B.M. Sherrill, *Prog. Part. Nucl. Phys.* **45** (2000) S171.
- [2] I. Tanihata, H. Hamagaki, O. Hashimoto, Y. Shida, N. Yoshikawa, K. Sugimoto, O. Yamakawa, and T. Kobayashi, *Phys. Rev. Lett.* **55** (1985) 2676.
- [3] P.G. Hansen, A.S. Jensen, and B. Jonson, *Ann. Rev. Nucl. Sci.* **45** (1995) 591.
- [4] J. Dobaczewski, I. Hamamoto, W. Nazarevich, and J.A. Sheikh, *Phys. Rev. Lett.* **72** (1994) 981.
- [5] I. Tanihata, *Prog. Part. Nucl. Phys.* **35** (1995) 505.

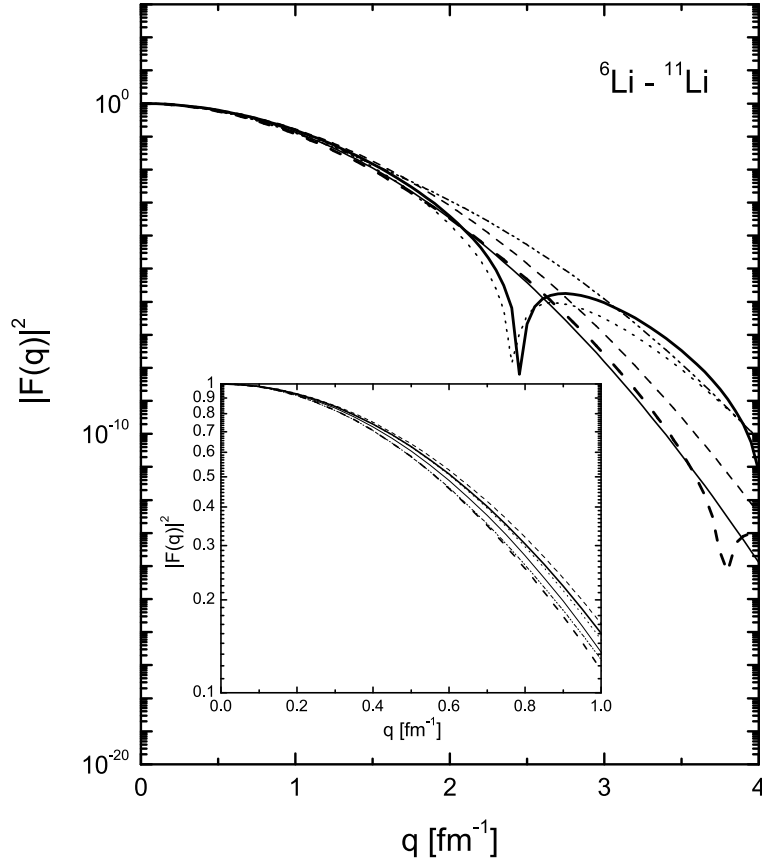


Figure 3: Charge form factors from Eq. (4): a) for ${}^6\text{Li}$ calculated using the experimental $\rho_{ch}(r)$ [36, 37] (dotted line), using the COSMA density [11, 12] (dash-two-dotted line), and using the LSSM density [35] (thick dashed line), and b) for ${}^{11}\text{Li}$ calculated using the the COSMA density [11] (thin solid line), the point-proton form factor $F_{point}(q)$ calculated using the point-proton density from [11] (thin dashed line), and using the LSSM density [35] (thick solid line).

- [6] Yu.Ts. Oganessian, V.I. Zagrebaev, and J.S. Vaagen, *Phys. Rev. Lett.* **82** (1999) 4996.
- [7] Yu.Ts. Oganessian, V.I. Zagrebaev, and J.S. Vaagen, *Phys. Rev.* **C60** (1999) 044605.
- [8] M.D. Cortina-Gil, P. Roussel-Chomaz, N. Alamanos, J. Barette, W. Mittig, F. Auger, Y. Blumenfeld, J.M. Casandjian, M. Chartier, V. Fekou-Youmbi, B. Fernandez, N. Frascaria, A. Gillibert, H. Laurent, A. Lepine-Szily, N.A. Orr, V. Pascalon, J.A. Scarpaci, J.L. Sida, and T. Saomijarvi, *Nucl. Phys.* **A616** (1997) 215c.
- [9] A. Lagoyannis, F. Auger, A. Musumarra, N. Alamanos, E.C. Pollacco, A. Pakou, Y. Blumenfeld, F. Braga, M.La. Commara, A. Drouart, G. Fioni, A. Gillibert, E. Khan, V. Lapoux, W. Mittig, S. Ottini-Hustache, D. Pierroutsakou, M. Romoli, P. Roussel-Chomaz, M. Sandoli, D. Santonocito, J.A. Scarpaci, J.L. Sida, T. Saomijarvi, S. Karataglidis, and K. Amos, *Phys. Lett.* **B518** (2001) 27.
- [10] M.D. Cortina-Gil, P. Roussel-Chomaz, N. Alamanos, J. Barette, W. Mittig, F. Auger, Y. Blumenfeld, J.M. Casandjian, M. Chartier, V. Fekou-Youmbi, B. Fernandez, N. Fraskaria, A. Gillibert, H. Laurent, A. Lepine-Szily, N.A. Orr, V. Pascalon, J.A. Scarpaci, J.L. Sida, and T. Saomijarvi, *Phys. Lett.* **B371** (1996) 14.

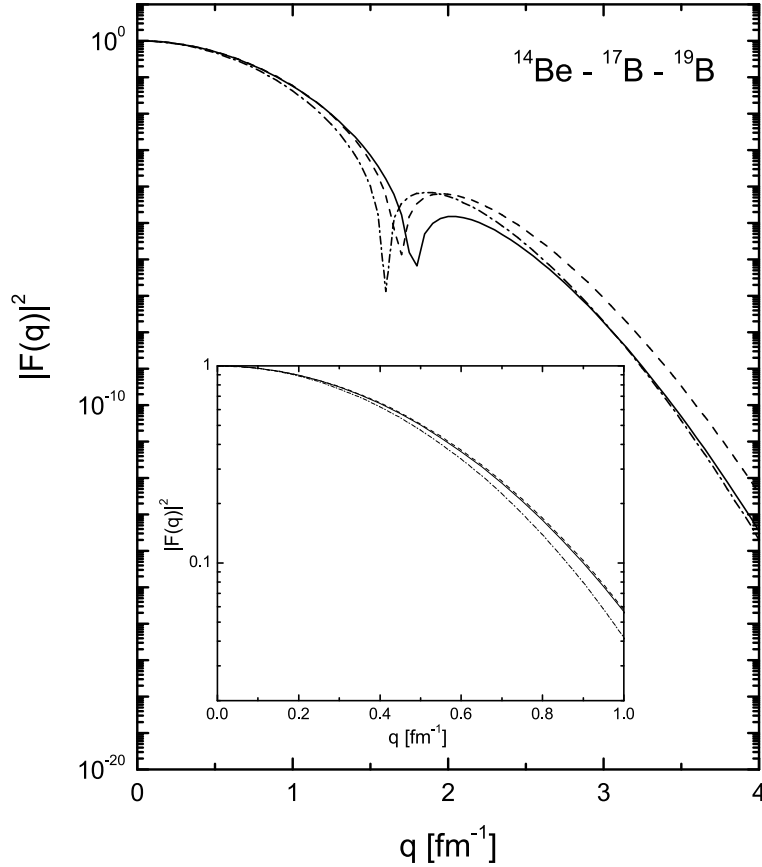


Figure 4: Charge form factors from Eq. (4) for ^{14}Be (solid line), ^{17}B (dashed line) and ^{19}B (dash-dotted line) calculated using the point-proton densities from [38].

- [11] A.A. Korshennikov, E.A. Kuzmin, E.Yu. Nikolskii, C.A. Bertulani, O.V. Bochkarev, S. Fukuda, T. Kobayashi, S. Momota, B.G. Novatskii, A.A. Ogloblin, A. Ozawa, V. Pribora, I. Tanihata, and K. Yoshida, *Nucl. Phys.* **A616** (1997) 189c.
- [12] A.A. Korshennikov, E.Yu. Nikolskii, C.A. Bertulani, S. Fukuda, T. Kobayashi, E.A. Kuzmin, S. Momota, B.G. Novatskii, A.A. Ogloblin, A. Ozawa, V. Pribora, I. Tanihata, and K. Yoshida, *Nucl. Phys.* **A617** (1997) 45.
- [13] G.M. Ter-Akopian et al., "Fundamental issues in elementary", in *Proceedings of Symposium in Honor and Memory of Michael Danos*, Bad Honnef, Germany, 2000, edited by W. Greiner (EP Systema, Debrecen, 2001), p. 371.
- [14] L.L. Chulkov, C.A. Bertulani, and A.A. Korshennikov, *Nucl. Phys.* **A587** (1995) 291.
- [15] A.A. Korshennikov, K. Yoshida, D.V. Alexandrov, N. Aoi, Y. Doki, N. Inabe, M. Fujimaki, T. Kobayashi, H. Kumagai, C.-B. Moon, E.Yu. Nikolskii, M.M. Obuti, A.A. Ogloblin, A. Ozawa, S. Shimoura, T. Suzuki, Y. Watanabe, and M. Yanokura, *Phys. Lett.* **B316** (1993) 38.
- [16] R. Crespo, J.A. Tostevin, and R.C. Johnson, *Phys. Rev.* **C51** (1995) 3283.
- [17] M. Avrigeanu, G.S. Anagnostatos, A.N. Antonov, and J. Giapitzakis, *Phys. Rev.* **C62** (2000) 017001.

- [18] M. Avrigeanu, G.S. Anagnostatos, A.N. Antonov, and V. Avrigeanu, *Int. J. Mod. Phys.* **E11** (2002) 249.
- [19] N. Anantaraman, H. Toki, and G. Bertsch, *Nucl. Phys.* **A398** (1983) 279.
- [20] G.R. Satchler and W.G. Love, *Phys. Rep.* **55** (1979) 183; G.R. Satchler, *Direct Nuclear Reactions* (Clarendon, Oxford, 1983).
- [21] Dao T. Khoa and W. von Oertzen, *Phys. Lett.* **B304** (1993) 8; *ibid.* **342** (1995) 6; Dao T. Khoa, W. von Oertzen, and H.G. Bohlen, *Phys. Rev.* **C49** (1994) 1652; Dao T. Khoa, W. von Oertzen, and A.A. Ogloblin, *Nucl. Phys.* **A602** (1996) 98; Dao T. Khoa and G.R. Satchler, *Nucl. Phys.* **A668** (2000) 3.
- [22] I. Tanihata, D. Hirata, T. Kobayashi, S. Shimoura, K. Sugimoto, and H. Toki, *Phys. Lett.* **B289** (1992) 261.
- [23] M.V. Zhukov, B.V. Danilin, D.V. Fedorov, J.M. Bang, I.J. Thompson, and J.S. Vaagen, *Phys. Rep.* **231** (1993) 151.
- [24] M.V. Zhukov, A.A. Korshennikov, and M.H. Smedberg, *Phys. Rev.* **C50** (1994) R1.
- [25] P.J. Dortmans, K. Amos, S. Karataglidis, and J. Raynal, *Phys. Rev.* **C58** (1998) 2249.
- [26] S. Karataglidis, P.J. Dortmans, K. Amos, and C. Bennhold, *Phys. Rev.* **C61** (2000) 024319.
- [27] K. Amos, in *Proceedings of 9th Conference on Nuclear Reaction Mechanisms*, Varenna, 2000, edited by E. Gadioli (Ricerca Scientifica ed Educazione Permanente, Milano, 2000), p. 51.
- [28] G.D. Alkhazov, M.N. Andonenko, A.V. Dobrovolsky, P. Egelhof, G.E. Gavrilov, H. Geissel, H. Irnich, A.V. Khanzadeev, G.A. Korolev, A.A. Lobodenko, G. Münzenberg, M. Mutterer, S.R. Neumaier, F. Nickel, W. Schwab, D.M. Selivestrov, T. Suzuki, J.P. Theobald, N.A. Timofeev, A.A. Vorobyov, and V.I. Yatsoura, *Phys. Rev. Lett.* **78** (1997) 2313.
- [29] T. de Forest, Jr. and J.D. Walecka, *Adv. Phys.* **15** (1966) 1.
- [30] G.D. Alkhazov, V.V. Anisovich, and P.E. Volkovyckii, in *Diffractional interaction of hadrons with nuclei at high energies*, Nauka, Leningrad, 1991, p. 94.
- [31] V.V. Burov and V.K. Lukyanov, Preprint JINR, R4-11098, 1977, Dubna.
- [32] W.F. Hornyak, *Nuclear Structure*, (Academic, New York, 1975), p. 240.
- [33] P.J. Karol, *Phys. Rev.* **C11** (1975) 1203.
- [34] H. De Vries, C.W. De Jager, and C. De Vries, *At. Data Nucl. Data Tables* **36** (1987) 495.
- [35] S. Karataglidis, B.A. Brown, K. Amos, and P.J. Dortmans, *Phys. Rev.* **C55** (1997) 2826.
- [36] J.D. Patterson and R.J. Peterson, *Nucl. Phys.* **A717** (2003) 235.
- [37] E. Friedman, A. Gal, and J. Mares, *Nucl. Phys.* **A579** (1994) 518.
- [38] T. Suzuki, R. Kanungo, O. Bochkarev, L. Chulkov, D. Cortina, M. Fukuda, H. Geissel, M. Hellström, M. Ivanov, R. Janik, K. Kimura, T. Kobayashi, A.A. Korshennikov, G. Münzenberg, F. Nickel, A.A. Ogloblin, A. Ozawa, M. Pfützner, V. Pribora, H. Simon, B. Sitár, P. Strmen, K. Sumiyoshi, K. Sümmerer, I. Tanihata, M. Winkler, and K. Yoshida, *Nucl. Phys.* **A658** (1999) 313.

Table 1: Charge radii (in fm) and diffuseness (in fm) of the charge densities.

Nuclei	Charge rms	Diffuseness	Densities
${}^4\text{He}$	1.68	0.30	Exp. [34]
	1.81	0.41	Tanihata [22]
	2.03	0.44	LSSM [26]
${}^6\text{He}$	1.89	0.42	Tanihata [22]
	2.06	0.45	COSMA [11]
	2.08	0.49	LSSM [26]
${}^8\text{He}$	1.93	0.43	Tanihata [22]
	1.87	0.41	COSMA [11]
	2.04	0.45	LSSM [26]
${}^6\text{Li}$	2.57	0.54	Exp. [36, 37]
	2.57	0.52	COSMA [11]
	2.63	0.55	LSSM [35]
${}^{11}\text{Li}$	2.45	0.54	COSMA [11]
	2.51	0.57	LSSM [35]
${}^{14}\text{Be}$	2.87	0.64	Suzuki [38]
${}^{17}\text{B}$	2.84	0.60	Suzuki [38]
${}^{19}\text{B}$	2.98	0.63	Suzuki [38]